Integrating Voltage-Source Active Filters into Diode Front-End Rectifiers – Harmonic Mitigation and Power Factor Correction

Daniel Bernet and Marc Hiller
Elektrotechnisches Institut (ETI) - Power Electronic Systems
Karlsruhe Institute of Technology (KIT)
Kaiserstr. 12, 76131 Karlsruhe, Germany
daniel.bernet@kit.edu

Keywords

≪Active filter≫, ≪Harmonics≫, ≪Power quality≫, ≪Power factor correction≫, ≪Voltage Source Converter≫, ≪FACTs≫, ≪Static Synchronous Compensator (STATCOM)≫.

Abstract

The ongoing grid integration of power electronic based loads requires the increasing use of power filters in order to maintain a high power quality and stability. To address this challenge, conventional active and passive filters are commonly used to meet the harmonic limits defined by the grid code. They allow the mitigation of voltage and current harmonics, however the filter performance is often subject to a limited frequency range or a frequency dependent harmonic mitigation. This paper presents a novel control scheme with a significantly reduced frequency dependence of harmonic mitigation for a voltage-source active filter configuration. Although high control bandwidth and identification of individual harmonics are not required, the harmonics of a diode front-end rectifier can almost entirely be eliminated, while the active filter load is consistently limited to harmonic currents in steady state and transient operation. As a result, the parallel voltage-source active filter can be designed for a small share of the installed load power and constitutes a promising alternative to conventional power filters.

Introduction

The increased share of power electronic based loads significantly affects the power quality and stability of modern power grids and even may cause disruption to the power supply [1]. To limit the harmonic distortion caused by power electronics, power filters are commonly used to meet the harmonic requirements defined by the grid code. Due to the high-volume application, the design and optimization of passive and active power filters is addressed in a large number of research contributions. Passive filters classified in [2] are the most commonly used filter configuration, however their use is often subject to important disadvantages such as high costs, substantial additional losses, frequency dependence, and susceptibility to oscillation.

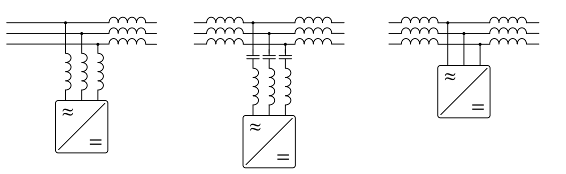

(a) Shunt (b) Hybrid (c) Voltage-Source

Fig. 1: Configurations of parallel active filters

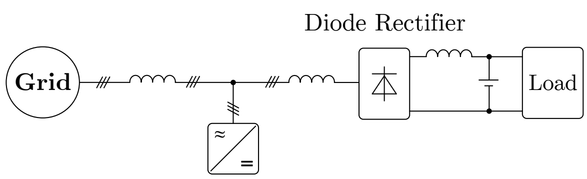

Fig. 2: Diode front-end rectifier with VS-AF

As future grid standards are likely to further tighten the harmonic limits, the aforementioned disadvantages associated with the use of passive filters may continue to increase.
Due to this development, active filters (AFs) can represent an attractive alternative to conventional passive filters. They use a power converter to reduce harmonics and can simultaneously provide fundamental reactive power for power factor correction [3]. Among the possible configurations of parallel AFs shown in Fig. 1, the shunt-AF in Fig. 1(a) is most commonly used in commercial applications. It is typically operated with harmonic current control in order to mitigate a number of individual harmonics [4–7].
To reduce the required converter power rating, a large number of AF topologies in combination with passive components according to Fig. 1(b) have been investigated in previous works and are commonly called hybrid-AFs [8–12]. For this topology, control schemes were presented which use the calculation of the total harmonic current to be compensated instead of detecting individual harmonics. However, the series-connected filter inductor and capacitor, which are often tuned to have low impedance at the targeted frequencies, can cause parameter sensitivity and frequency dependence of the harmonic mitigation.
A promising approach to increase the compensated frequency range and robustness to parameter deviations is the voltage-source active filter (VS-AF) shown in Fig. 1(c). The concept of parallel VS-AFs is used in [13] for a solid-state reactive power compensator. Therein, a dc-link voltage controlled two-level voltage-source converter (2L-VSC) allows a steady state power factor correction of a three-phase load by fundamental reactive power compensation. A current sensorless control of a 2L-VSC as VS-AF is introduced in [14, 15] for harmonic mitigation of a diode front-end rectifier based load. In [16], a VS-AF based on a dc-link voltage controlled multilevel inverter is used for harmonic mitigation of a nonlinear load and for supplying this load during grid voltage dips.
Since previous works have not focused on minimizing the load current of the VS-AF, it must be designed for a significant share of the load power in the applications described. Reducing the power rating could lower the cost of the VS-AF and allow it to operate at a higher switching frequency, resulting in a reduction in grid-side filter inductance and harmonic distortion of the grid current. Therefore, this contribution focuses on a highly dynamic VS-AF control for the application shown in Fig. 2, whose objective is to limit the VS-AF current to harmonic currents of the diode front-end rectifier in steady state and transient operation. This ensures that, to a good approximation, the VS-AF carries no fundamental current and can thus be designed for a significantly reduced power rating compared to the installed load power, enabling its use in highly integrated power electronic based loads.

Control

In order to enable the use of the VS-AF in a wide field of applications, a control scheme design is required that allows operation independent of the type of load. Unlike the hybrid converter topology introduced in [20, 21], where the integration of the VS-AF in a single converter system allows the use of a coupled control scheme, the decoupled operation requires the independent identification of all currents and voltages relevant to the VS-AF control.
Fig. 3 shows the single-phase equivalent circuit of a parallel VS-AF connected to a power line. It should be emphasized that the VS-AF is connected to the power line without a coupling impedance, whereby the voltage-source output characteristic leads to a defined busbar voltage $\underline{v}_{\mathrm{b}} = \underline{v}_{\mathrm{af}}$. For this reason, the grid voltage $\underline{v}_{\mathrm{g}}$ can be used for feed-forward control by the converter to ensure an accurate grid synchronization. As a result of the defined busbar voltage, the grid current

$$\underline{i}_{\mathrm{g}} = \frac{\underline{v}_{\mathrm{g}} - \underline{v}_{\mathrm{af}}}{\underline{Z}_{\mathrm{g}}} \tag{1}$$

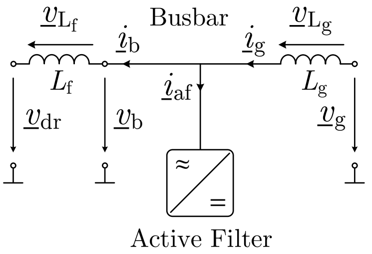

Fig. 3: Single-phase equivalent circuit of the VS-AF connected to a power line

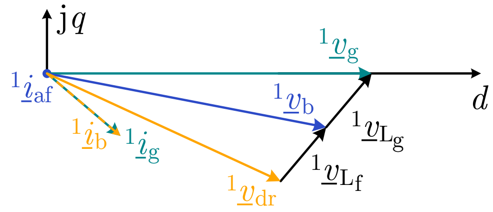

Fig. 4: Fundamental frequency complex vector diagram for ideal AF operation (schematic)

is determined by the grid voltage $\underline{v}_{\mathrm{g}}$, the VS-AF output voltage $\underline{v}_{\mathrm{af}}$ and the grid-side impedance $\underline{Z}_{\mathrm{g}} = \underline{Z}_{\Sigma} + \mathrm{j}\omega_{\mathrm{g}}L_{\mathrm{g}}$, where $\underline{Z}_{\Sigma}$ is the accumulated impedance of grid resources such as transmission lines and transformers. To allow a low power rating by ensuring that the VS-AF only reduces the injected grid harmonics and is not exchanging active or fundamental reactive power, the fundamental busbar current $^1\underline{i}_{\mathrm{b}}$ is used as grid current reference. This is identified by transforming the measured three-phase busbar current $\boldsymbol{i}_{\mathrm{b}}$ into $dq-$coordinates using a double-decoupled synchronous reference frame phase-locked-loop (DDSRF-PLL) [22] and filtering it with a moving average filter (MAF). The determination of the MAF window length has a significant impact on the harmonic and dynamic performance of the control and will be discussed in the next section.
Neglecting losses, Fig. 4 shows the fundamental frequency complex vector diagram for operation with minimized current load of the VS-AF. It should be emphasized that the sole objective of the VS-AF control is to ensure $^1\underline{i}_{\mathrm{g}} = {}^1\underline{i}_{\mathrm{b}}$ and thus minimize $^1\underline{i}_{\mathrm{af}}$ during steady state and transient operation. As a result, according to Kirchhoff's Current Law (KCL) at the connection node

$$\underline{i}_{\mathrm{af}} = {}^1\underline{i}_{\mathrm{g}} - {}^1\underline{i}_{\mathrm{b}} + \sum_{\nu=2}^{\infty} {}^{\nu}\underline{i}_{\mathrm{g}} - \sum_{\nu=2}^{\infty} {}^{\nu}\underline{i}_{\mathrm{b}} = \sum_{\nu=2}^{\infty} {}^{\nu}\underline{i}_{\mathrm{g}} - \sum_{\nu=2}^{\infty} {}^{\nu}\underline{i}_{\mathrm{b}} \tag{2}$$

with harmonic order $\nu = \{h \in \mathbb{N} | h \geq 2\}$, the VS-AF is inherently carrying the difference between grid- and load-side current harmonics, while the former are negligible for the use of an VS-AF with high switching frequency and high output voltage quality. Therefore, since neither the identification of individual harmonics, the measurement of high-frequency current ripple, nor a high control bandwidth are required for this purpose, conventional fundamental-frequency control based on PI-controllers can be used for the VS-AF control.
Although the VS-AF ideally only compensates harmonic reactive power, a small active current $^1i_{\mathrm{af,d}}$ is required in practice for power unit and auxiliary loss compensation. In addition, using AF topologies with distributed dc-links, unsymmetrical energy distributions in the converter can require a fundamental reactive current $^1i_{\mathrm{af,q}}$ in order to balance the converter cells [17]. According to the system equations resulting from the equivalent circuit in Fig. 3, additional output currents $^1i_{\mathrm{af,d}}$ and $^1i_{\mathrm{af,q}}$ can be attained by using additional output voltages $^1v_{\mathrm{b,q}}$ and $^1v_{\mathrm{b,d}}$, respectively. Since the VS-AF has no dc supply, an energy control performs the fundamental frequency current control to ensure a constant dc-link voltage and stable operation. The energy control is based on the separation of power components, as introduced in [17] for Modular Multilevel Converters (MMCs) and used for a parallel hybrid converter in [18, 19].

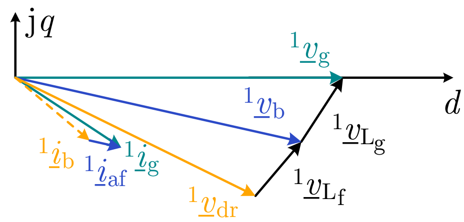

Fig. 5: Fundamental frequency complex vector diagram for AF operation with consideration of energy control (schematic)

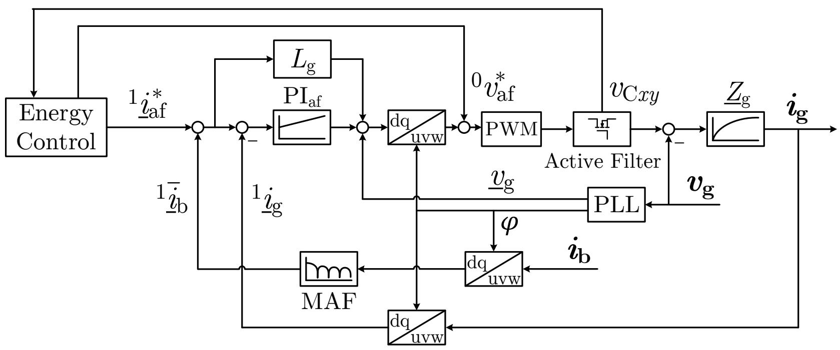

Fig. 6: Fundamental frequency VS-AF control scheme for mitigating current harmonics of diode front-end rectifiers

Fig. 5 shows the corresponding fundamental frequency complex vector diagram, which is not drawn to scale for better comprehension. It should be noted that due to the voltage dependence of many passive loads, a change in ${}^{1}\underline{v}_{\text{b}}$ will likely cause a simultaneous change in ${}^{1}\underline{i}_{\text{b}}$. However, since only a small change in voltage ${}^{1}\underline{v}_{\text{b}}$ is required for the VS-AF current ${}^{1}\underline{i}_{\text{af}}$, the resulting deviation of ${}^{1}\underline{i}_{\text{b}}$ is assumed to be negligible. The developed fundamental frequency control scheme of the parallel VS-AF is shown in Fig. 6.

Simulation

In Fig. 7, a nonlinear load composed of a 6-pulse diode front-end rectifier with a connected dc load is supplied by the low voltage grid, where typical dc loads are industrial electric drives or voltage dependent passive loads. To achieve a small harmonic distortion of the output voltage and a sinusoidal grid current, a Cascaded H-Bridge Active Filter (CHB AF) in star configuration according to [23] is used as the VS-AF. Simulation results are carried out for the grid and VS-AF parameters given in Table I. In addition, the diode front-end rectifier uses an ac-side filter inductance $L_{\text{f}} = 200\,\mu$H and a dc-link filter inductance $L_{\text{dc}} = 26\,\mu$H.

Table I: Simulation Parameters

	Parameter	Symbol	Value
Grid	Voltage	V_{g}	400 V
	Frequency	f_{g}	50 Hz
	Filter inductance	L_{g}	200 μH
VS-AF	No. of cells	n_{af}	12
	DC-link voltage	V_{C}	35 V
	Cell capacitance	C_{af}	6 mF
	Switching freq.	$f_{\text{sw,af}}$	12 kHz
	Sampling freq.	$f_{\text{s,af}}$	96 kHz
	Window length	n_{maf}	320
Load	AC-Inductance	L_{f}	200 μH
	DC-Inductance	L_{dc}	26 μH

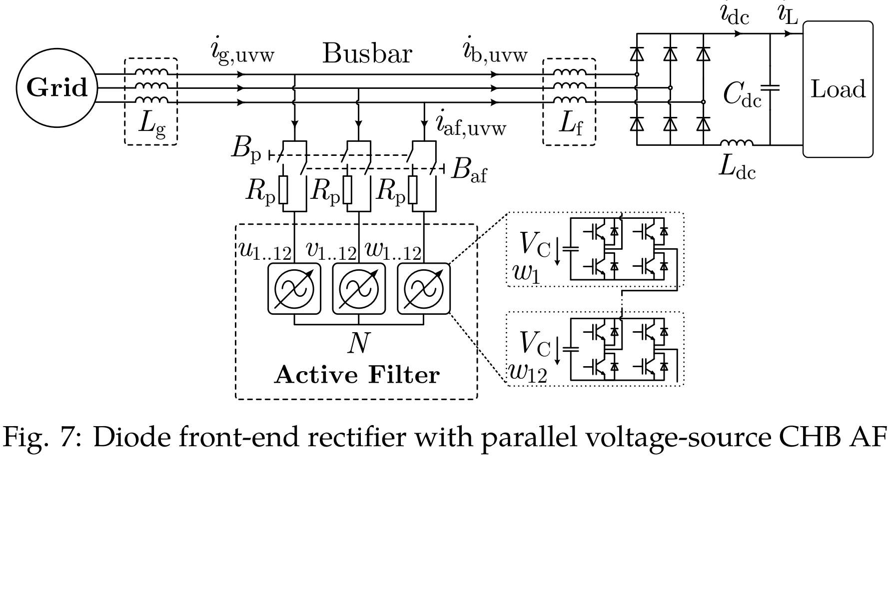

Fig. 7: Diode front-end rectifier with parallel voltage-source CHB AF

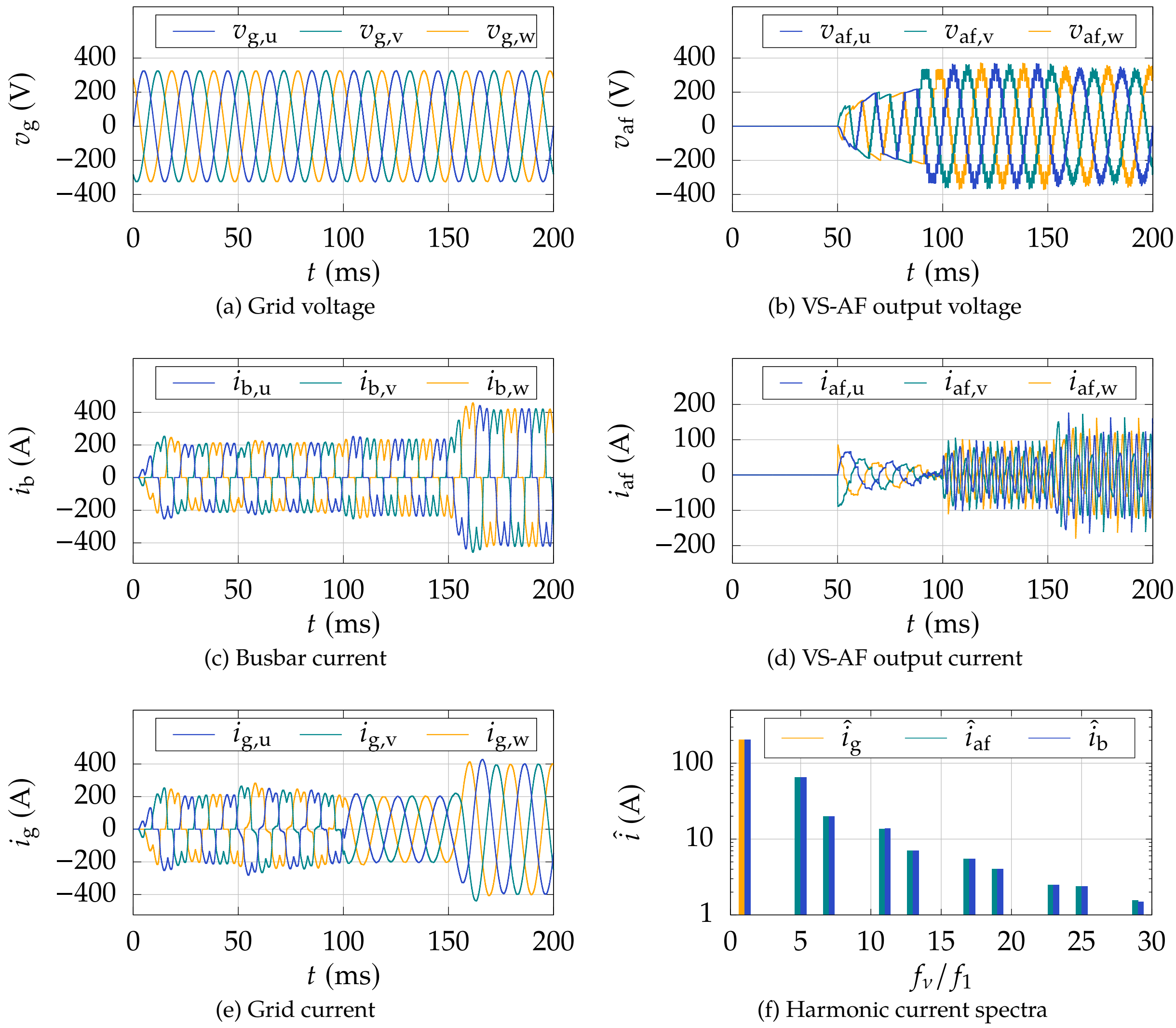

(a) Grid voltage (b) VS-AF output voltage

(c) Busbar current (d) VS-AF output current

(e) Grid current (f) Harmonic current spectra

Fig. 8: Simulation results of the diode front-end rectifier with parallel voltage-source CHB AF

Fig. 8 shows the resulting voltage and current waveforms of the busbar, VS-AF and grid. Initially, the dc load current rises and causes a highly distorted busbar current in Fig. 8(c) with an amplitude of approximately $\hat{i}_b$ = 200 A. Since the VS-AF is not yet connected, high harmonic currents typical for diode front-end rectifiers are injected into the grid. The VS-AF is precharged beginning at t = 50 ms by closing breaker B_p and is connected to the busbar at t = 100 ms by closing breaker B_{af} (see Fig. 7). As can be seen in Fig. 8(d), the VS-AF compensates the substantial harmonic distortion of the busbar current and thereby significantly reduces the injected current harmonics, leading to a sinusoidal grid current in Fig. 8(e). Fig. 8(f) shows the harmonic current spectra of the grid, VS-AF and busbar. Therein, the high harmonic busbar currents of the 5th and 7th order caused by the diode front-end rectifier can be seen, leading to a significant harmonic distortion of THD_b = 34.8 %. However, since the VS-AF topology and control allow frequency independent harmonic mitigation, the grid current corresponds in good approximation to a fundamental current with THD_g = 0.3 %. Due to the significant harmonic currents, the required electrical power ratio of VS-AF and diode front-end rectifier at this operating point is 26.6 %. According to the phase-shift between the grid voltage in Fig. 8(a) and current in Fig. 8(e), the power factor is 0.96.

At t = 150 ms, the dc load current increases to i_L = 360 A, resulting in an increased busbar current amplitude and load power of approximately $\hat{i}_b$ = 400 A and 200 kVA, respectively. Even in transient operation, the VS-AF accurately compensates the busbar current ripple and thereby allows the grid current to remain sinusoidal. Although the current ripple is still reduced as compared to the total busbar current, an increase of the VS-AF current load can be seen in Fig. 8(d) due to the load dependent current harmonics of the diode front-end rectifier. However, since the required VS-AF current rating is not increasing proportionally with the load current, the electrical power ratio decreases to 20 % at this operating point. The busbar current distortion results in $\mathrm{THD_b} = 26.5\,\%$, while the harmonic distortion of the grid current remains constant at $\mathrm{THD_g} = 0.3\,\%$. Since the phase-shift between grid voltage and current increases with the load, the power factor decreases to 0.93.

Discussion of the MAF window length

To achieve a high control accuracy and harmonic performance, the determination of the MAF window length requires consideration of the lowest harmonic orders to be expected in the busbar current. If the window length does not correspond to the period duration of a harmonic current or an integer multiple of it, this harmonic current passes the MAF. According to (1), assuming a sinusoidal grid voltage, the injected grid current harmonics depend on the VS-AF output voltage, which is determined primarily by the current reference, the number of voltage levels, the modulation-index and the switching frequency. KCL at the connection node according to (2) reveals that the VS-AF inherently compensates busbar current harmonics that are not contained in the grid current. If a harmonic current passes the MAF in consequence of a disadvantageous window length, it contributes to the current reference and thereby will be contained in the grid current. However, in order to achieve a tradeoff with the dynamic performance of the VS-AF, the maximum current slope during transient operation needs to be considered and limits the maximum window length.
Fig. 9 shows the measured busbar currents transformed into $dq-$coordinates. According to the harmonic current spectra in Fig. 8(f), the 5^{th} and 7^{th} harmonics are the lowest harmonic orders of the three-phase busbar current. Since the 5^{th} harmonic is a negative sequence in three-phase coordinates, it corresponds to the 6^{th} harmonic in $dq-$coordinates. At the same time, the 7^{th} harmonic, which is a positive sequence in contrast, is also corresponding to the 6^{th} harmonic in $dq-$coordinates. Since larger harmonics of the diode front-end rectifier in Fig. 8(f) correspond to integer multiples of the 6^{th} harmonic in $dq-$coordinates, optimal window lengths exist that allow the MAF in good approximation to eliminate all harmonics from the measured busbar current. To achieve this, it is advantageous to set the MAF window length to the period duration of the 6^{th} harmonic or integer multiples of it. Considering a sampling frequency of $f_{\mathrm{s,af}} = 96\,\mathrm{kHz}$ according to Table I, this corresponds to a MAF window length of 320 or integer multiples of it. The harmonic currents of the filtered busbar current and the grid current are shown in Fig. 10 as a function of the MAF window length. As expected, the harmonic currents for MAF window lengths of 320 or integer multiples of it are almost entirely eliminated from the measured busbar current and thus from the grid current. Although window lengths of 640 and more offer higher noise reduction, a window length of 320 is a suitable tradeoff to achieve high dynamic

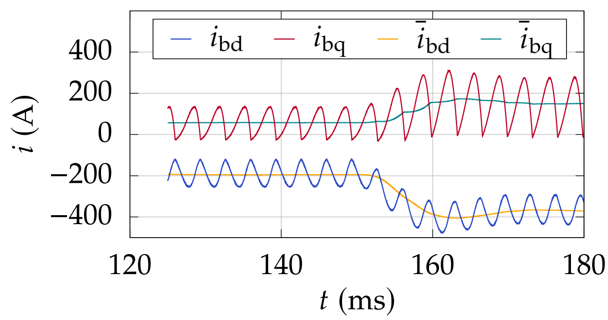

Fig. 9: Busbar currents in $dq-$coordinates: i_{bd} and i_{bq} are unfiltered, $\bar{i}_{\mathrm{bd}}$ and $\bar{i}_{\mathrm{bq}}$ are filtered using a MAF with a window length of 320

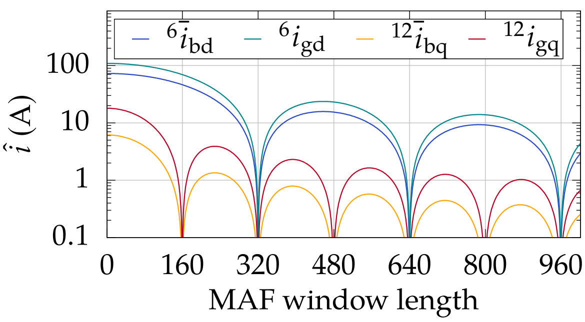

Fig. 10: Harmonic currents as a function of the MAF window length: Filtered busbar currents $\bar{i}_{\mathrm{bd}}$ and $\bar{i}_{\mathrm{bq}}$, grid currents i_{gd} and i_{gq}

performance at the same time. This can be seen in Fig. 9, where the filtered currents $\bar{i}_{\mathrm{bd}}$ and $\bar{i}_{\mathrm{bq}}$ correspond in good approximation to the moving average values of the measured currents i_{bd} and i_{bq} in steady state and transient operation. Since $\bar{i}_{\mathrm{bd}}$ and $\bar{i}_{\mathrm{bq}}$ are used as references for the grid current control, the VS-AF current, corresponding to the difference of the grid current and the busbar current, is consistently limited to current harmonics of the diode front-end rectifier.

Power Factor Correction

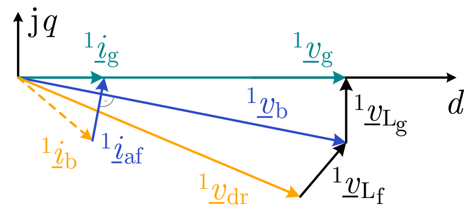

Fig. 11: Fundamental frequency complex vector diagram for ideal AF operation with power factor correction (schematic)

In addition to harmonic mitigation, AFs can also provide fundamental reactive power and thus maintain a grid-side power factor close to unity (e.g. [13, 24, 25]). Since the proposed VS-AF directly controls the grid current with conventional fundamental frequency control in $dq-$coordinates, providing fundamental reactive power can be achieved by determining the reactive grid current reference to zero. The corresponding fundamental frequency complex vector diagram is shown in Fig. 11, which neglects the VS-AF losses and is not drawn to scale for better comprehension. In practice, the slight change in the VS-AF output voltage would result in a slight change in the load power of the diode front-end rectifier. However, the change is assumed to be small and, moreover, the required active grid current is adjusted in this case by the energy control of the VS-AF.

The simulation results using harmonic mitigation and power factor correction are shown in Fig. 12. It can be seen that the grid voltage in Fig. 12(a) and the grid current in Fig. 12(d) are in phase to a very good approximation, indicating an unity power factor. On the other hand, the VS-AF current in Fig. 12(c) is increased compared to the operation without power factor correction in Fig. 8(d). This increases the required electrical power ratio of VS-AF and diode front-end rectifier at this operating point by 6.5 % to 33.1 %.

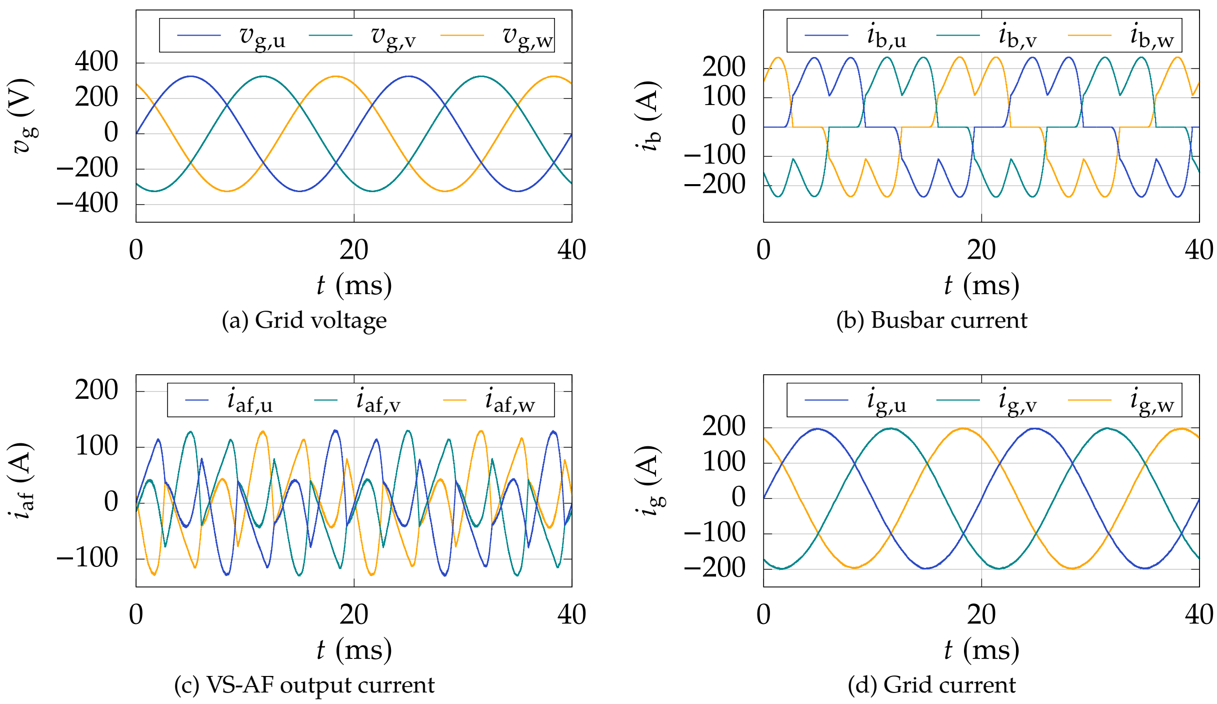

Fig. 12: Simulation results using harmonic mitigation and power factor correction

Conclusion

A novel control scheme for an AF configuration with voltage-source output characteristics is presented in this contribution. The VS-AF is connected in parallel to a power line without a coupling impedance and allows the mitigation of current harmonics at a reduced power rating. Since only the fundamental frequency current of the power line needs to be identified, the compensable harmonic orders are theoretically not limited to below the Nyquist frequency. Moreover, unlike conventional AFs based on harmonic current control, the parallel VS-AF mitigates not only distinct harmonic frequencies but most of the harmonic current distortions, however high control bandwidth and the identification of individual harmonics are not required. In order to illustrate the potential for improving the harmonic performance of nonlinear loads, a CHB AF is used as grid-side output filter of a 6-pulse diode front-end rectifier. Despite considerable 5^{th} and 7^{th} order current harmonics, the introduced control scheme allows the VS-AF to mitigate almost the entire current distortion caused by the load, leading to a sinusoidally-shaped grid current with a total harmonic distortion of only 0.3 %. The required electrical power ratio of VS-AF and diode front-end rectifier is 26.6 % and 20 % for loads of 100 kVA and 200 kVA, respectively. In addition to harmonic mitigation, power factor correction by providing fundamental reactive power can be easily implemented in the control scheme, but this requires an increased power ratio due to the additional fundamental current load of the VS-AF.

References

[1] X. Wang and F. Blaabjerg, "Harmonic Stability in Power Electronic-Based Power Systems: Concept, Modeling, and Analysis", *IEEE Transactions on Smart Grid* 10.3 (May 2019), pp. 2858–2870.

[2] R. N. Beres, X. Wang, M. Liserre, F. Blaabjerg, and C. L. Bak, "A Review of Passive Power Filters for Three-Phase Grid-Connected Voltage-Source Converters", *IEEE Journal of Emerging and Selected Topics in Power Electronics* 4.1 (Mar. 2016), pp. 54–69.

[3] B. Singh, K. Al-Haddad, and A. Chandra, "A review of active filters for power quality improvement", *IEEE Transactions on Industrial Electronics* 46.5 (1999), pp. 960–971.

[4] P. Mattavelli, "A closed-loop selective harmonic compensation for active filters", *IEEE Transactions on Industry Applications* 37.1 (2001), pp. 81–89.

[5] M. Liserre, R. Teodorescu, and F. Blaabjerg, "Multiple harmonics control for three-phase grid converter systems with the use of PI-RES current controller in a rotating frame", *IEEE Transactions on Power Electronics* 21.3 (May 2006), pp. 836–841.

[6] C. Lascu, L. Asiminoaei, I. Boldea, and F. Blaabjerg, "Frequency Response Analysis of Current Controllers for Selective Harmonic Compensation in Active Power Filters", *IEEE Transactions on Industrial Electronics* 56.2 (Feb. 2009), pp. 337–347.

[7] E. Kontos, G. Tsolaridis, R. Teodorescu, and P. Bauer, "High Order Voltage and Current Harmonic Mitigation Using the Modular Multilevel Converter STATCOM", *IEEE Access* 5 (2017), pp. 16684–16692.

[8] H. Fujita and H. Akagi, "A practical approach to harmonic compensation in power systems-series connection of passive and active filters", *IEEE Transactions on Industry Applications* 27.6 (1991), pp. 1020–1025.

[9] B. Singh, V. Verma, A. Chandra, and K. Al-Haddad, "Hybrid filters for power quality improvement", *IEE Proceedings - Generation, Transmission and Distribution* 152.3 (2005), p. 365.

[10] H. Akagi and R. Kondo, "A Transformerless Hybrid Active Filter Using a Three-Level Pulsewidth Modulation (PWM) Converter for a Medium-Voltage Motor Drive", *IEEE Transactions on Power Electronics* 25.6 (June 2010), pp. 1365–1374.

[11] S. Rahmani, A. Hamadi, K. Al-Haddad, and L. A. Dessaint, "A Combination of Shunt Hybrid Power Filter and Thyristor-Controlled Reactor for Power Quality", *IEEE Transactions on Industrial Electronics* 61.5 (May 2014), pp. 2152–2164.

[12] H. Bai, X. Wang, P. C. Loh, and F. Blaabjerg, “An Active Trap Filter for Switching Harmonic Attenuation of Low-Pulse-Ratio Inverters”, *IEEE Transactions on Power Electronics* 32.12 (Dec. 2017), pp. 9078–9092.

[13] G. Joos, L. Moran, and P. Ziogas, “Performance analysis of a PWM inverter VAr compensator”, *IEEE Transactions on Power Electronics* 6.3 (July 1991), pp. 380–391.

[14] M. Routimo, M. Salo, and H. Tuusa, “Current sensorless control of a voltage-source active power filter”, in *Twentieth Annual IEEE Applied Power Electronics Conference and Exposition, 2005. APEC 2005.* IEEE.

[15] M. Routimo, M. Salo, and H. Tuusa, “Control method to improve the transient performance of a current sensorless active power filter”, in *Nordic Workshop on Power and Industrial Electronics (NORpie), Lund, Sweden*, 2006.

[16] M. Ortuzar, R. Carmi, J. Dixon, and L. Moran, “Voltage-source active power filter based on multilevel converter and ultracapacitor DC link”, *IEEE Transactions on Industrial Electronics* 53.2 (Apr. 2006), pp. 477–485.

[17] J. Kolb, F. Kammerer, M. Gommeringer, and M. Braun, “Cascaded Control System of the Modular Multilevel Converter for Feeding Variable-Speed Drives”, *IEEE Transactions on Power Electronics* 30.1 (Jan. 2015), pp. 349–357.

[18] L. Stefanski, D. Bernet, M. Schnarrenberger, C. Rollbühler, A. Liske, and M. Hiller, “Cascaded H-Bridge based Parallel Hybrid Converter - A novel topology for perfectly sinusoidal high power voltage sources”, in *IECON 2019 - 45th Annual Conference of the IEEE Industrial Electronics Society*, IEEE, Oct. 2019.

[19] D. Bernet, L. Stefanski, and M. Hiller, “Integrating Voltage-Source Active Filters into Grid-Connected Power Converters Modeling, Control and Experimental Verification”, *IEEE Transactions on Power Electronics* (2021), doi: 10.1109/TPEL.2021.3075068.

[20] D. Bernet, L. Stefanski, R. Schwendemann, C. Rollbühler, and M. Hiller, “Grid-Connected Voltage Source Converters with integrated Multilevel-Based Active Filters”, in *2018 IEEE Energy Conversion Congress and Exposition (ECCE)*, IEEE, Sept. 2018.

[21] D. Bernet and M. Hiller, “Grid-connected medium-voltage converters with parallel voltage-source active filters”, *IET Electric Power Applications* (May 2019).

[22] R. Teodorescu, M. Liserre, and P. Rodriguez, *Grid Converters for Photovoltaic and Wind Power Systems*, John Wiley & Sons, Feb. 10, 2011, 418 pp.

[23] D. Bernet, R. Schwendemann, L. Stefanski, and M. Hiller, “A Highly Integrated 25-Level Cascaded H-Bridge Active Filter for the Mitigation of High Order Current Harmonics”, in *PCIM Europe digital days 2021; International Exhibition and Conference for Power Electronics, Intelligent Motion, Renewable Energy and Energy Management*, 2021, pp. 1–8.

[24] A. Chandra, B. Singh, B. Singh, and K. Al-Haddad, “An improved control algorithm of shunt active filter for voltage regulation, harmonic elimination, power-factor correction, and balancing of nonlinear loads”, *IEEE Transactions on Power Electronics* 15.3 (May 2000), pp. 495–507.

[25] J. Chen, X. Zhang, and C. Wen, “Harmonics Attenuation and Power Factor Correction of a More Electric Aircraft Power Grid Using Active Power Filter”, *IEEE Transactions on Industrial Electronics* 63.12 (Dec. 2016), pp. 7310–7319.